



## TRAJECTORY TRACKING CONTROL OF A TWO WHEELED SELF-BALANCING ROBOT BY USING SLIDING MODE CONTROL

<sup>1,\*</sup> Mustafa DOĞAN , <sup>2</sup> Ümit ÖNEN 

<sup>1</sup>AVL Research and Engineering, Istanbul, TÜRKİYE

<sup>2</sup>Necmettin Erbakan University, Engineering Faculty, Mechatronics Engineering Department, Konya, TÜRKİYE

<sup>1</sup>[mustafa.dogan@avl.com](mailto:mustafa.dogan@avl.com), <sup>2</sup>[uonen@erbakan.edu.tr](mailto:uonen@erbakan.edu.tr)

### Highlights

- Trajectory tracking control of a two wheeled self-balancing robot by using Sliding Mode Control (SMC) was realized.
- The performance of the SMC controller has been examined under five different cases including external disturbance and various parameter uncertainties and compared with PID and LQR methods.
- Chattering problem inherent in the SMC method was eliminated by employing tangent hyperbolic (tanh) switching function instead of signum function.
- Results showed that, PID control is extremely sensitive to disturbance inputs and parameter changes, and the LQR controller provides a much better performance than the PID control in terms of response speed and robustness. The results also showed that the proposed SMC controller not only offer as good performance as the LQR controller in terms of response speed, but it is extremely robust and almost insensitive to disturbance inputs and excessive parameter changes.



## TRAJECTORY TRACKING CONTROL OF A TWO WHEELED SELF-BALANCING ROBOT BY USING SLIDING MODE CONTROL

<sup>1,\*</sup> Mustafa DOĞAN , <sup>2</sup> Ümit ÖNEN 

<sup>1</sup>AVL Research and Engineering, Istanbul, TÜRKİYE

<sup>2</sup>Necmettin Erbakan University, Engineering Faculty, Mechatronics Engineering Department, Konya, TÜRKİYE

<sup>1</sup>mustafa.dogan@avl.com, <sup>2</sup>uonen@erbakan.edu.tr

(Received: 26.01.2024; Accepted in Revised Form: 30.05.2024)

**ABSTRACT:** Two-Wheeled Self-Balancing Robots are widely used in various fields today. These systems have a highly unstable nature due to their underactuated structures. On the other hand, parameter uncertainties and external disturbances significantly affect their control performance. The best way to deal with parameter uncertainties that can easily lead controllers to instability is to use robust control methods. Dealing with these uncertainties is particularly crucial in control of underactuated and unstable systems such as Two-Wheeled Self-Balancing Robots. In this study, trajectory tracking control of a two wheeled self-balancing robot by using Sliding Mode Control (SMC) was realized. The chattering problem inherent in the SMC method was eliminated by employing tangent hyperbolic ( $\tanh$ ) switching function instead of signum function. The performance of the SMC controller has been examined under five different cases including external disturbance and various parameter uncertainties and compared with PID and LQR methods. The results showed that the SMC method is much more insensitive to parameter changes than the PID and LQR methods. It has also been observed that all three controllers maintain their stability against disturbance inputs, but the SMC method offers a better control performance.

**Keywords:** Sliding Mode Control, Two Wheeled Self Balancing Robot, Trajectory Tracking

**ÖZ:** İki Tekerlekli Kendini Dengeleyen Robotlar günümüzde çeşitli alanlarda yaygın olarak kullanılmaktadır. Bu sistemler eksik tahrikli yapıları nedeniyle oldukça kararsız bir yapıya sahiptirler. Öte yandan parametre belirsizlikleri ve dış etkenler, kontrol performanslarını önemli ölçüde etkilemektedir. Kontrolcülerini kolayca kararsızlığa sürükleyebilecek parametre belirsizlikleri ile başa çıkmanın en iyi yolu gürbüz kontrol yöntemleri kullanmaktır. Bu belirsizliklerle başa çıkmak, özellikle İki Tekerlekli Kendini Dengeleyen Robotlar gibi eksik-tahrikli ve kararsız sistemlerin kontrol problemlerinde çok önemlidir. Bu çalışmada, bozucu giriş ve parametre belirsizliklerine karşı Kayan Kipli Kontrol (KKK) yöntemi ile yörünge takibi üzerinde çalışılmıştır. KKK yönteminin yapısından kaynaklanan çatırtı problemi, işaret fonksiyonu yerine tanjant hiperbolik ( $\tanh$ ) anahtarlama fonksiyonu kullanılarak ortadan kaldırılmıştır. KKK kontrolcüsünün performansı, bozucu giriş ve farklı parametre belirsizliklerini içeren beş farklı senaryo için incelemiş, PID ve LQR yöntemleri ile karşılaştırılmıştır. Sonuçlar, KKK yönteminin parametre değişimlerine karşı PID ve LQR yöntemlerinden çok daha duyarsız olduğunu göstermiştir. Ayrıca bozucu girişlere karşı üç kontrolcüsünün de kararlılığını koruduğu ancak KKK yönteminin daha iyi bir kontrol performansı sunduğu görülmüştür.

**Anahtar Kelimeler:** Kayan Kipli Kontrol, İki Tekerlekli Denge Robotu, Yörünge Takibi.

### 1. INTRODUCTION

Underactuated systems refer to systems equipped with a limited number of actuators or sensors. In such systems, the number of degrees of freedom is greater than the number of actuators or sensors used. Despite their advantages such as low cost, energy efficiency and simplicity, underactuated systems have some disadvantages in terms of control.

\*Corresponding Author: Mustafa DOĞAN, [mustafa.dogan@avl.com](mailto:mustafa.dogan@avl.com)

Two-wheeled self-balancing robots have a highly unstable dynamics with their nonlinear structure. In addition, other factors such as parameter changes, damping, friction, external disturbances make the control of such systems more difficult. The best way to overcome these challenges is to use robust controllers. In the relevant literature, several different approaches have been proposed for the control of two-wheeled self-balancing robots.

Linear control methods with simple mathematical models are frequently preferred due to their easy applicability. Linear controllers such as PID controller [1], Linear Quadratic Regulator (LQR) [2], Linear Quadratic Gaussian (LQG) [3], State-Feedback [4], Cascade controller [5] can be used to control two-wheeled self-balancing robots. These controllers can provide very satisfactory performance in some systems under certain conditions. However, since these controllers use linearised models, they are very sensitive to parameter uncertainties. In addition, due to their structure, they may be insufficient against external disturbances.

As an alternative to classical linear controllers, smart control methods such as Fuzzy Logic Controller (FLC) [6], FLC-PID [7], FLC-LQR [8] are widely using. Smart control methods can provide more adaptivity than classic approaches. However, they still cannot provide robustness in parameter uncertainty conditions.

Adaptive control algorithms have been presented to adapt to changing conditions over time. Various adaptive control methods such as Reinforcement Learning [9], Machine Learning [10], Artificial Neural Networks [11], Fuzzy Logic Neural Networks NN-FLC [12] stand out with less model dependency and adaptive structure. Despite their advantages, design and training of large networks in these approaches can be quite complex. High computational power and large data set requirements during training of artificial neural networks make it difficult to apply these methods.

Model Predictive Control (MPC) [13] which is based on predicting system behaviour using system models, can provide robustness against system uncertainties in the control of complex systems. However, the success of this approach depends on very precisely modelled system dynamics. Difficulties in modelling complex and nonlinear systems limit the success of the controller. Optimisation-based  $H_2$  [14],  $H_\infty$  [15] approaches can provide robustness against the disturbances and parameter uncertainties with an accurate model. The biggest disadvantage of these controllers is that they can be effective in a limited working area with defined cost functions.

Lyapunov Controllers [16] are successful in stability; however, they may not be satisfactory enough to meet performance expectations for systems that require precise control. Backstepping Control [17] and Active Disturbance Rejection Control (ADRC) [18] are also have robust characteristics.

The Sliding Mode Control (SMC) approach is a control method known for its robustness against the disturbances and system uncertainties. Although the Conventional SMC method is insensitive to matched disturbances, but it is sensitive to unmatched disturbances. The state observer-based SMC [19] can ensure the robustness of the controller against the unmatched disturbances. The major disadvantage of the SMC is chattering problem. In the most general definition, chattering is the rapid changes of the control signal in high-frequency sawtooth form. This is caused by the switching function in the structure of the SMC. The chattering problem can be eliminated with Neural Network based SMC [20]. However, high computational demanding and the need for a comprehensive dataset are disadvantages of this approach.

In this study, the trajectory tracking control of a two-wheeled self-balancing robot was discussed. First, kinematic and dynamic models of the system are presented. Then, a Sliding Mode controller with tangent hyperbolic switching function was designed. In order to evaluate the response speed and robustness of the designed controller, simulation studies were carried out using five different scenarios with different disturbance inputs and parameter changes. For comparing the performance of the SMC controller, PID and LQR control were also applied to the system and the results were presented comparatively.

## 2. MATERIAL AND METHODS

Simplified model of a two-wheeled self-balancing robot is seen in Figure 1. The system consists of a chassis and a pendulum-shaped body balanced by two wheels. It is an underactuated system with two

inputs and three outputs. The right and left wheel torques are the system inputs while the  $x$  -  $y$  coordinates and  $\theta$  angle of the body relative to vertical ( $z$ ) axis are the system outputs. This system is quite difficult to control since the position, orientation and vertical angle of the body must be controlled only by the torques applied to wheels. In order to achieve a precise control, the kinematic and dynamic models of the system must be obtained accurately.

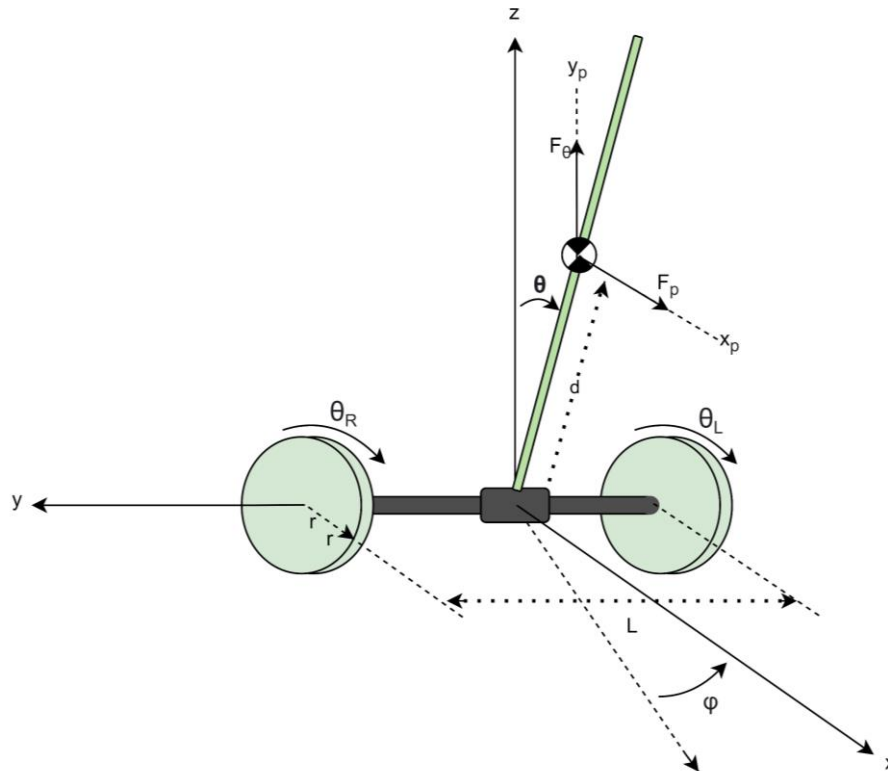


Figure 1. Simplified model of a two-wheeled self-balancing robot

### 2.1. Kinematic Model of The Two-Wheeled Self-Balancing Robot

In order to describe all movements of the system, generalized coordinates can be selected as follows.

$$q = [X_c \ Y_c \ \varphi \ \theta \ \theta_R \ \theta_L]^T \quad (1)$$

In this expression,  $X_c$  and  $Y_c$ , are the position of the centre of mass,  $\varphi$  is the angle of the robot in the  $x$ - $y$  plane,  $\theta$  is the angle between the body and the vertical ( $z$ ) axis,  $\theta_R$  and  $\theta_L$  are the right and left wheel angles, respectively. These coordinates are clearly seen in Figure 2.

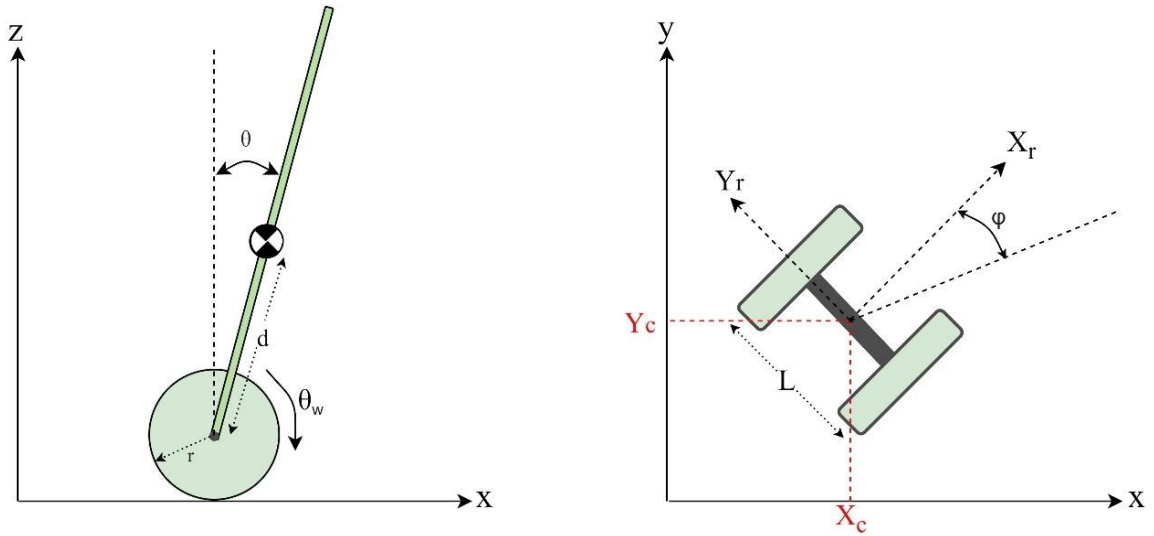


**Figure 2.** Generalized coordinates of the two-wheeled self-balancing robot

There are two different constraints for the system considered in this study. First, the wheels do not slide laterally. Secondly, the wheels are in pure rolling, that is, the entire rotational movement turns into translation. Therefore, by defining  $l=L/2$ , the constraint equations can be written as follows.

$$\dot{y} \cos\varphi - \dot{x} \sin\varphi = 0 \tag{2}$$

$$\begin{aligned} \dot{x} \cos\varphi - \dot{y} \sin\varphi + l\dot{\varphi} - r\dot{\theta}_r &= 0 \\ \dot{x} \cos\varphi - \dot{y} \sin\varphi - l\dot{\varphi} - r\dot{\theta}_l &= 0 \end{aligned} \tag{3}$$

Linear and angular velocities of the system can be defined respectively as;  $v = r(\dot{\theta}_r + \dot{\theta}_l)/2$  and  $\omega = r(\dot{\theta}_r - \dot{\theta}_l)/L$ . If the necessary arrangements are made in (2) and (3) using these definitions, the kinematic model of the system is obtained as follows.

$$\begin{bmatrix} \dot{x} \\ \dot{y} \\ \dot{\varphi} \end{bmatrix} = \begin{bmatrix} \cos\varphi & 0 \\ \sin\varphi & 0 \\ 0 & 1 \end{bmatrix} \begin{bmatrix} v \\ \omega \end{bmatrix} \tag{4}$$

**2.2. Dynamic Model of The Two-Wheeled Self-Balancing Robot**

In this study, the dynamic model of two-wheeled self-balancing robot presented by Junfeng and Wangying [21] was used. State-space representation of the system can be defined as  $\dot{x} = Ax + Bu$  and shown as follow,

$$x = \begin{bmatrix} \dot{x}_r \\ \dot{x}_l \\ \dot{\theta} \\ \dot{\varphi} \\ \dot{\varphi} \end{bmatrix} = \begin{bmatrix} 0 & 1 & 0 & 0 & 0 & 0 \\ 0 & 0 & A_{23} & 0 & 0 & 0 \\ 0 & 0 & 0 & 1 & 0 & 0 \\ 0 & 0 & A_{43} & 0 & 0 & 0 \\ 0 & 0 & 0 & 0 & 0 & 1 \\ 0 & 0 & 0 & 0 & 0 & 0 \end{bmatrix} \begin{bmatrix} x_r \\ x_l \\ \theta \\ \varphi \\ \varphi \end{bmatrix} + \begin{bmatrix} 0 \\ B_2 \\ 0 \\ B_4 \\ 0 \\ B_6 \end{bmatrix} \begin{bmatrix} C_l \\ C_r \end{bmatrix} \tag{5}$$

where  $C_l$  and  $C_r$  are the left end right wheel torques respectively. This wheel torques can be transformed into the  $C_\theta$  and  $C_\varphi$  for decoupling purpose as follow.

$$\begin{bmatrix} C_l \\ C_r \end{bmatrix} = \begin{bmatrix} 0.5 & 0.5 \\ 0.5 & -0.5 \end{bmatrix} \begin{bmatrix} C_\theta + u_d \\ C_\varphi \end{bmatrix} \tag{6}$$

In this equation,  $u_d$  is the external disturbance. The matrix elements in Equation (5) can be defined as follows:

$$\begin{aligned} A_{23} &= g \left( 1 - \frac{4}{3} d \frac{M_p}{Q} \right), & A_{43} &= g \frac{M_p}{Q} \\ B_2 &= \frac{4dP}{3Q} - \frac{1}{M_p d}, & B_4 &= -\frac{P}{Q} \\ B_6 &= \frac{6}{(9M_r + M_p)RL} \end{aligned} \quad (7)$$

where

$$Q = \frac{1}{3} \frac{M_p(M_p + 6M_r)d}{(M_p + \frac{3}{2}M_r)R}, \quad P = \frac{1}{d} + \frac{M_p}{M_p + \frac{3}{2}M_r}$$

In these equations,  $M_w$  and  $M_p$  is the mass of the wheel and body respectively,  $R$  is the wheel radius,  $d$  is the distance between the wheel axis and centre of mass and  $L$  is the distance between wheels.

### 2.3. Kinematic Controller

Controllers that calculate the kinematic movements required for a robot to reach the desired position are called kinematic controllers. A kinematic controller is needed to perform of trajectory control. The kinematic controller calculates the movements required for a robot to reach the desired position by converting the desired trajectory motions into new outputs in terms of angular and linear velocity. Kinematic controller design is based on the kinematic model. Equation (4) can be rearranged as follows:

$$\begin{bmatrix} v \\ \omega \end{bmatrix} = \begin{bmatrix} \cos\varphi & \sin\varphi \\ -\frac{1}{d} \sin\varphi & \frac{1}{d} \cos\varphi \end{bmatrix} \begin{bmatrix} \dot{x} \\ \dot{y} \end{bmatrix} \quad (8)$$

By defining  $\tilde{x} = x_d - x$  and  $\tilde{y} = y_d - y$  and adding the controller gains  $k_x, k_y > 0$  and saturation constants  $I_x, I_y \in \mathbb{R}$  into equation, the kinematic controller can be obtained as below [22].

$$\begin{bmatrix} v_d \\ \omega_d \end{bmatrix} = \begin{bmatrix} \cos\varphi & \sin\varphi \\ -\frac{1}{d} \sin\varphi & \frac{1}{d} \cos\varphi \end{bmatrix} \begin{bmatrix} \dot{x}_d + I_x \tanh\left(\frac{k_x}{I_x} \tilde{x}\right) \\ \dot{y}_d + I_y \tanh\left(\frac{k_y}{I_y} \tilde{y}\right) \end{bmatrix} \quad (9)$$

### 2.4. Sliding Mode Controller

In applied control problems, there is always mismatching between the real system and the mathematical model. It's caused by factors such as unmodelled system dynamics, uncertainties in system parameters and disturbing external forces. In addition to model mismatches, if the system is exposed to intense disturbing forces, it will be very difficult to control such systems with classical closed-loop methods. At this point, robust controllers come into play [23].

SMC is a robust control approach that can provide stability guarantee against system uncertainties and disturbances. Before starting the SMC design, some arrangements should be made on the system model. By defining  $f_1 = A_{23}$ ,  $f_2 = A_{43}$ ,  $f_3 = \dot{\varphi}$ ,  $g_1 = B_2$ ,  $g_2 = B_4$ ,  $g_3 = B_6$ ,  $T_v = C_\theta$ ,  $T_\omega = C_\varphi$  in Equation

(5) and making the necessary arrangements, the dynamic equation of the system can be written in a new form as follows.

$$\begin{aligned}\ddot{x} &= f_1\theta + g_1T_v \\ \ddot{\theta}_p &= f_2\theta + g_2T_v \\ \ddot{\varphi} &= f_3 + g_3T_\omega\end{aligned}\quad (10)$$

Where  $T_v$  and  $T_\omega$  corresponds to control inputs for separated subsystems, and  $x_d, y_d, \varphi_d$  are desired positions, so the error dynamics of the system can be expressed as follows:

$$\begin{aligned}\dot{e}_1 &= e_2 \\ \dot{e}_2 &= \ddot{x} - \ddot{x}_d \\ \dot{e}_3 &= e_4 \\ \dot{e}_4 &= \ddot{\theta} - \ddot{\theta}_d \\ \dot{e}_5 &= e_6 \\ \dot{e}_6 &= \ddot{\varphi} - \ddot{\varphi}_d\end{aligned}\quad (11)$$

The SMC method will move the system dynamics towards the defined sliding surface. This movement of the controller is called reaching mode. The time until the reaching mode is called the reaching time. As soon as the system dynamics reaches the sliding surface, it starts the sliding motion. Sliding motion is called sliding mode. Sliding surfaces that move  $e_2, e_4$  and  $e_6$  errors towards to zero when  $t \rightarrow \infty$  can be defined as follows.

$$\begin{aligned}s_1 &= c_1e_1 + e_2 \\ s_2 &= c_2e_3 + e_4 \\ s_3 &= c_3e_5 + e_6\end{aligned}\quad (12)$$

The coefficients  $c_1, c_2, c_3 > 0$  in the defined sliding surfaces are called slope constants. The reaching time is related to the slope of the sliding surfaces. Therefore, these coefficients directly affect the control performance and should be chosen carefully. In order to obtain control signals, derivation of the Equation (12) can be written as follow.

$$\begin{aligned}\dot{s}_1 &= c_1\dot{e}_1 + \dot{e}_2 = \ddot{x} - \ddot{x}_d + c_1\dot{e}_1 \\ \dot{s}_2 &= c_2\dot{e}_3 + \dot{e}_4 = \ddot{\theta} - \ddot{\theta}_d + c_2\dot{e}_3 \\ \dot{s}_3 &= c_3\dot{e}_5 + \dot{e}_6 = \ddot{\varphi} - \ddot{\varphi}_d + c_3\dot{e}_5\end{aligned}\quad (13)$$

A SMC consists of two parts which called switching and equivalent. Switching part is a signum function, and is responsible for moving the system variables towards to sliding surface.  $\dot{s}_1, \dot{s}_2, \dot{s}_3$  terms in Equation (13) correspond to switching function. Switching function can be premised with defining controller gains as  $\eta_1, \eta_2, \eta_3 > 0$  as follow.

$$\begin{aligned}u_{sw1} &= \dot{s}_1 = -\eta_1 \operatorname{sgn}(s_1) \\ u_{sw2} &= \dot{s}_2 = -\eta_2 \operatorname{sgn}(s_2) \\ u_{sw3} &= \dot{s}_3 = -\eta_3 \operatorname{sgn}(s_3)\end{aligned}\quad (14)$$

Equivalent control occurs in condition when the system has reached to the sliding phase. This condition can be also defined as  $\dot{s}_1, \dot{s}_2, \dot{s}_3 = 0$ . Equation (11) and Equation (13) can be re-written as follow.

$$\begin{aligned}c_1\dot{e}_1 + \ddot{x} - \ddot{x}_d &= 0 \\ c_2\dot{e}_3 + \ddot{\theta} - \ddot{\theta}_d &= 0 \\ c_3\dot{e}_5 + \ddot{\varphi} - \ddot{\varphi}_d &= 0\end{aligned}\quad (15)$$

If Equation (15) arranged by using the Equation (10) then,

$$\begin{aligned} c_1 \dot{e}_1 + f_1 \theta + g_1 T_{v1} - \ddot{x}_d &= 0 \\ c_2 \dot{e}_3 + f_2 \theta + g_2 T_{v2} - \ddot{\theta}_d &= 0 \\ c_3 \dot{e}_5 + f_3 \varphi + g_3 T_\omega - \ddot{\varphi}_d &= 0 \end{aligned} \quad (16)$$

where  $T_{v1}$  and  $T_{v2}$  corresponds to torque forces related with coupled  $x$  and  $\theta$  inputs. The equivalent control term can be obtained by re-arranging Equation (16) as follows,

$$\begin{aligned} u_{eq1} &= \frac{\ddot{x}_d - c_1 \dot{e}_1 - f_1 \theta}{g_1} \\ u_{eq2} &= \frac{\ddot{\theta}_d - c_2 \dot{e}_3 - f_2 \theta}{g_2} \\ u_{eq3} &= \frac{\ddot{\varphi}_d - c_3 \dot{e}_5 - f_3 \varphi}{g_3} \end{aligned} \quad (17)$$

Finally, SMC control signal can be obtained with re-arrange Equation 10, 13 and 15 as follow.

$$\begin{aligned} T_{v1} &= \frac{\ddot{x}_d - c_1 \dot{e}_1 - \eta_1 \text{sgn}(s_1) - f_1 \theta}{g_1} \\ T_{v2} &= \frac{\ddot{\theta}_d - c_2 \dot{e}_3 - \eta_2 \text{sgn}(s_2) - f_2 \theta}{g_2} \\ T_\omega &= \frac{\ddot{\varphi}_d - c_3 \dot{e}_5 - \eta_3 \text{sgn}(s_3) - f_3 \varphi}{g_3} \end{aligned} \quad (18)$$

Control signals with control gains  $\eta_1, \eta_2, \eta_3 > 0$  can be obtained as above. It can be expressed as  $T_v = k_{VCSMC}(T_{v2} - T_{v1})$  and  $T_\omega = k_{\omega CSMC} T_\omega$  where  $k_{VCSMC}$  and  $k_{\omega CSMC}$  are the controller gain constants. Tangent hyperbolic (tanh) function is used instead of sign to prevent chattering. The obtained control signals can be modelled on Simulink as shown in Figure 3.

A Lyapunov function candidate in the form of  $V = \frac{1}{2}s$  is defined to perform stability analyse. According to the Lyapunov theorem, for a system to be stable, the condition  $\dot{V} \leq 0$  must be ensured.

$$\begin{aligned} \dot{V}_1 &= s_1 \dot{s}_1 = s_1(\ddot{x} - \ddot{x}_d + c_1 \dot{e}_1) = -\eta_1 |s_1| \leq 0 \\ \dot{V}_2 &= s_2 \dot{s}_2 = s_2(\ddot{\theta} - \ddot{\theta}_d + c_2 \dot{e}_3) = -\eta_2 |s_2| \leq 0 \\ \dot{V}_3 &= s_3 \dot{s}_3 = s_3(\ddot{\varphi} - \ddot{\varphi}_d + c_3 \dot{e}_5) = -\eta_3 |s_3| \leq 0 \end{aligned} \quad (19)$$

Equation (19) shows that all three controller signals ensure the Lyapunov stability condition. In other words, the designed controllers will lead the error signal in the system to zero in time. Sliding Mode Control strategy and general schematic of the closed loop system is given in Figure 3.



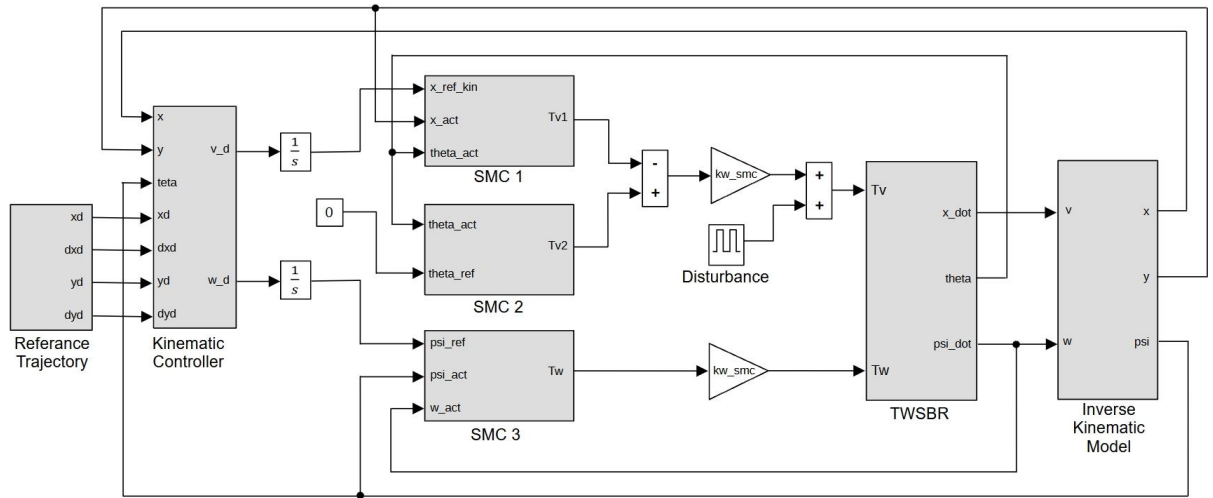


Figure 3. SMC - Closed Loop Block Diagram of the System

$\dot{x}$ ,  $\theta$ , and  $\varphi$  control variables are controlling respectively with SMC 1, SMC 2 and SMC 3 given in Figure 3. Detailed block diagram for SMC 1, SMC 2 and SMC 3 can be seen in Figure 4.

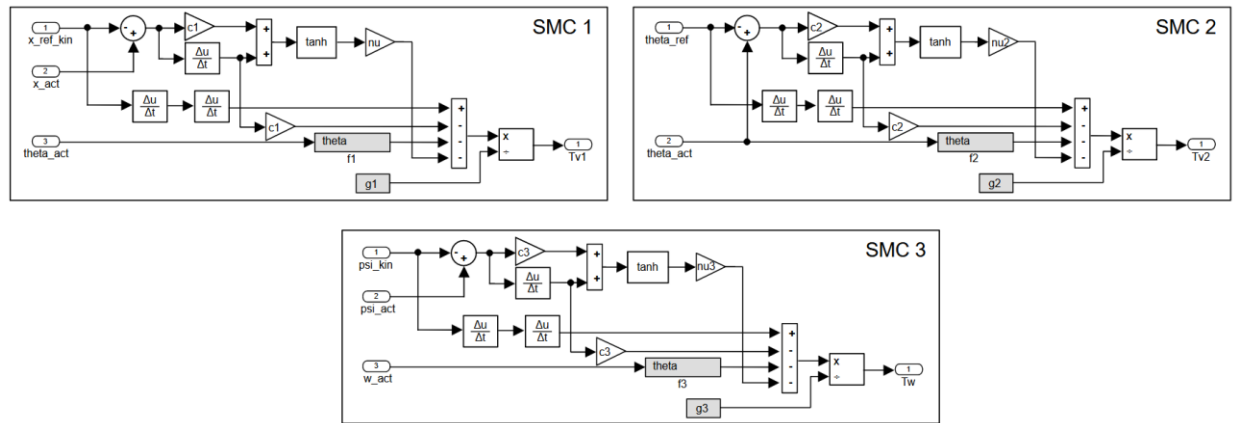


Figure 4. SMC Control Scheme

### 2.5. PID Control

PID is the abbreviation of “Proportional-Integral-Derivative” terms. While PID control can give good control performance in linear systems, it is not very satisfactory in dealing with non-linear systems. However, it is one of the most frequently used methods due to its easy design and applicability. The mathematical representation of the PID controller can be expressed as follows [24].

$$u(t) = K_p e(t) + K_i \int e(t) dt + K_d \frac{de}{dt} \tag{20}$$

In the Eq. 21.  $K_p$ ,  $K_i$  ve  $K_d$  gains respectively corresponds to proportional, integral and derivative part of the controller.  $e(t)$  corresponds to error inputs by time. The integral term corresponds to the integral of the error value and produces a control signal that corrects the total error. The term derivative refers to the derivative of the error value and produces a control signal that responds to rapidly changing errors. In other words, the proportional term refers to the current error, the integral term refers to the sum of past errors, and the derivative term refers to the prediction of future errors [25]. PID controller schematics can be seen in Figure 5.

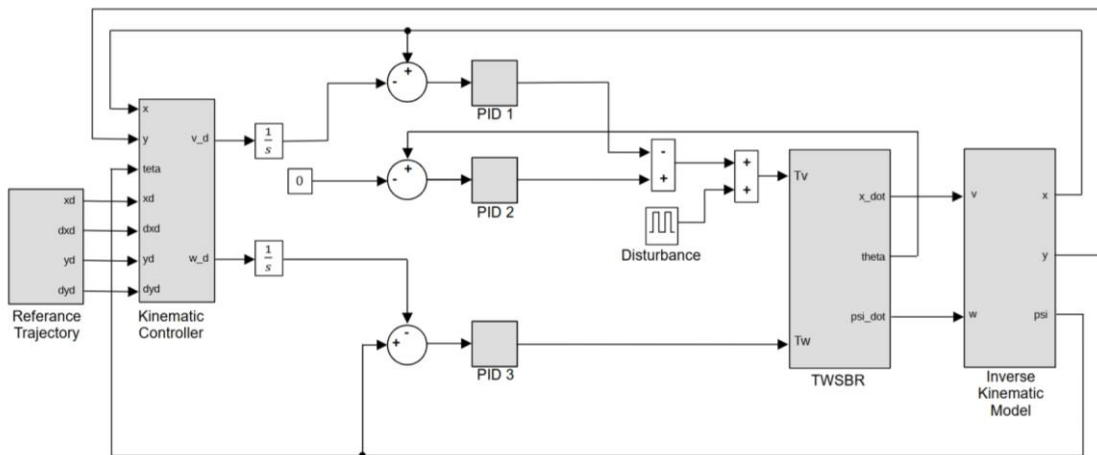


Figure 5. PID Closed Loop Control Schematic

2.6. LQR Control

The Linear Quadratic Regulator (LQR) is one of the optimal control methods frequently used today. In the LQR method, it is aimed to obtain an optimum control signal by using the performance index and the state variables of the system [26].

$$J = \frac{1}{2} \int_0^{\infty} (x^T Q x + u^T R u) dt \tag{21}$$

Performance index J which obtained using system state variables as  $\dot{x} = Ax + Bu$  and  $u = -Kx$  system inputs is given in Eq. 21. K is gain matrice and define as  $K = R^{-1}B^T P$ . Q and R diagonal matrices and P is a symmetrical matrix which can be obtained from Ricatti Equation given in Eq. 22.

$$PA + A^T - PBR^{-1}P + Q = 0 \tag{22}$$

The aim of the LQR method is to minimize the performance index J with using Q and R parameters. The Q matrix represents the speed of reaching the reference and the R parameter represents the amount of energy to be consumed. LQR control schematics can be seen in Figure 6.

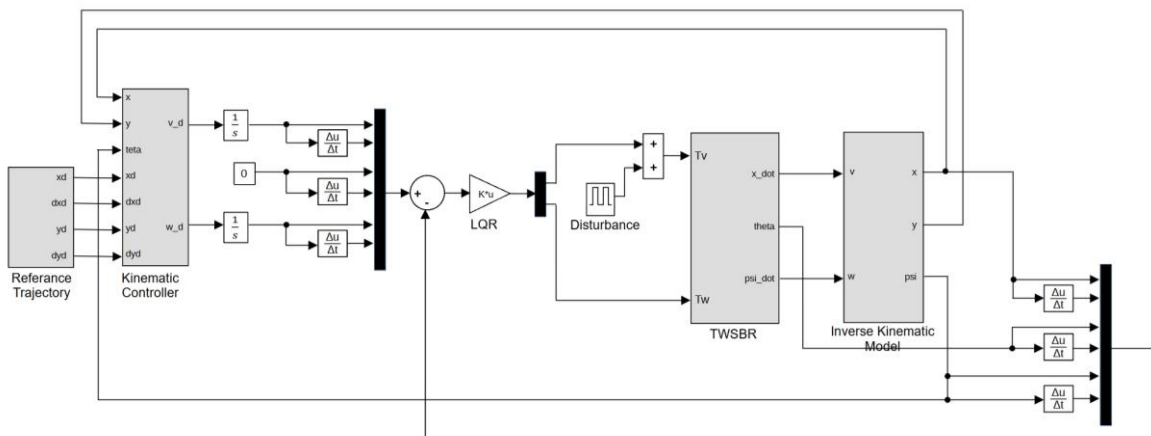


Figure 6. LQR Closed Loop Control Schematic

### 3. RESULTS AND DISCUSSION

In order to evaluate the response speed and robustness of the designed controller, simulation studies were carried out using five different scenarios having different disturbance inputs and parameter changes. PID and LQR control are also applied to the system to compare the performance of the proposed SMC controller. Simulation studies were carried out in MATLAB/Simulink. An infinite type of trajectory was used as a reference and the simulation time was determined as 150 seconds. System parameters are given in Table 1. All the SMC, PID and LQR controller parameters are determined by using trial-and-error method and given in Table 2.

**Table 1.** Physical Parameters of the System

Parameter	Description	Value
R	Wheel diameter	0.1 m
L	Distance between wheels	0.3 m
D	Distance of pendulum centre of gravity to shaft	0.45 m
g	Gravity force	9.8 m/s <sup>2</sup>
M <sub>p</sub>	Mass of the pendulum	3 kg
M <sub>w</sub>	Mass of the wheels	0.5 kg

**Table 2.** Controller Parameters

Kinematic Controller	$k_x, k_y = 4, I_x, I_y = 0.025$		
SMC	$k_{vCSMC} = 50, k_{\omega CSMC} = 1$	$C_1 = 1, C_2 = 10, C_3 = 5$	$\eta_1 = 3.5, \eta_2 = 11, \eta_3 = 1$
PID	$K_{P1} = -2, K_{I1} = -4, K_{D1} = -4$	$K_{P2} = -2, K_{I2} = -4, K_{D2} = -4$	$K_{P3} = -2, K_{I3} = -4, K_{D3} = -4$
LQR	$K = \begin{bmatrix} -27 & -51 & -334 & -23 & 0 & 0 \\ 0 & 0 & 0 & 0 & 10 & 1 \end{bmatrix}$		

**Case 1:** In the first simulation study, performances of the controllers are tested under ideal conditions without any disturbance or parameter changes and the results are given in Figure 5 – Figure 8. All the controllers showed a successful trajectory tracking performance by quickly providing the desired position and orientation as seen in Figure 7 and Figure 8. However, while the SMC and LQR controllers reached the reference velocity quickly at the beginning of the movement, the PID controller gave a very oscillatory and late response as seen in Figure 9. For the PID control, this fluctuation in the velocity caused the body to make an oscillatory movement and reach the equilibrium quite late as seen in Figure 10. Although the LQR control gave a successful result in terms of body angle, the SMC control showed the best performance. On the other hand, the SMC control produced much more aggressive torques than the others at the beginning of the movement, but it quickly stabilized as seen in Figure 10. Moreover, thanks to tanh switching function, there is no chattering in the SMC control signal.

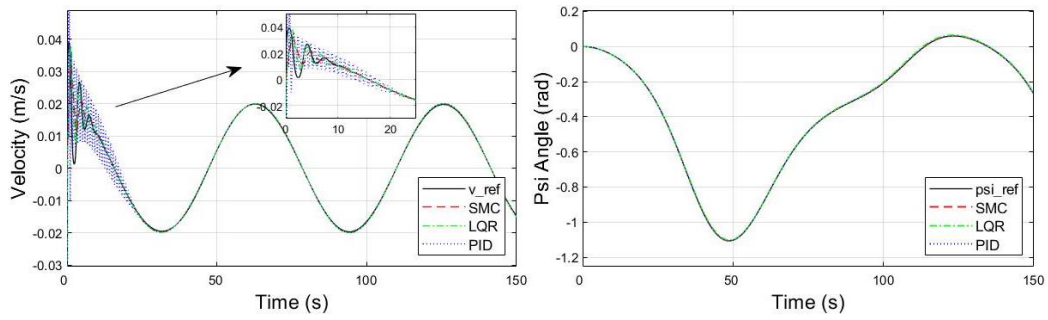


Figure 7. Velocity and movement angle ( $\psi$ ) of the robot (Case 1)

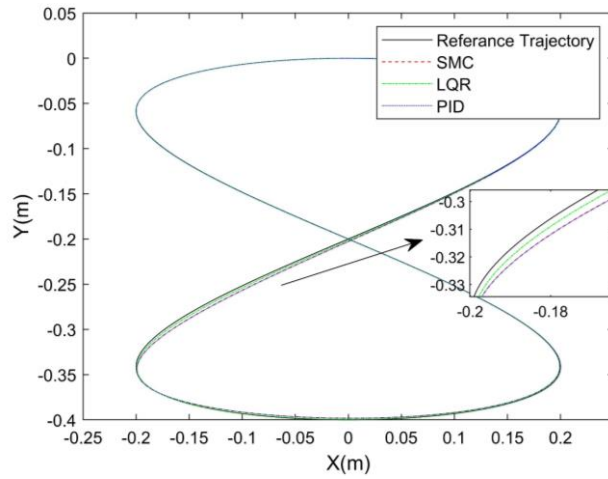


Figure 8. Trajectory tracking (Case 1)

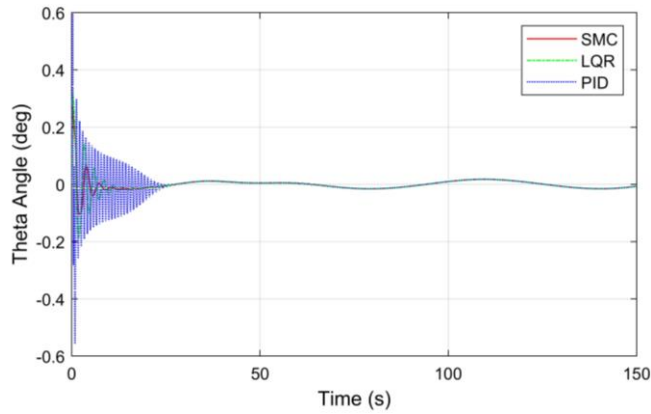


Figure 9. Body ( $\theta$ ) Angle (Case 1)

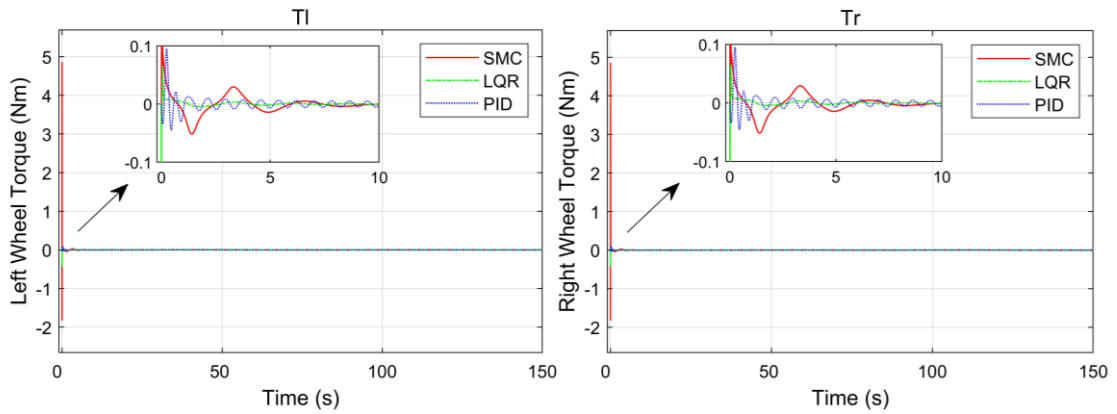


Figure 10. Wheel torques (Case 1)

In the following cases, disturbance input and parameter changes were applied to the system to examine the robustness of the controllers.

**Case 2:** In this case, only the 0.5 Nm impulse signal seen in Figure 11 was applied to the control input of the system for 1 second as a disturbance and no changes have been made to the system parameters. Disturbance input applied in coupled  $\dot{x}$  and  $\dot{\theta}$  control output and can be seen in Figure 3.

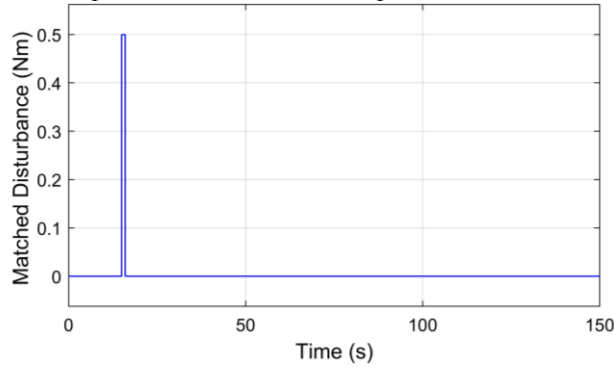


Figure 11. Disturbance signal applied to the system

In the presence of the disturbance, the trajectory tracking performance of the SMC and LQR control methods are quite close to each other. It can be seen from Figure 13 that the SMC and LQR controllers are much more insensitive to disturbance input than the PID controller. Additionally, while a limited speed fluctuation occurs in the LQR and SMC controllers after the disturbance input, these fluctuations are quite high in the PID controller as seen in Figure 12. As a result of velocity fluctuations, the maximum body angle reaches 1.5 degrees in the PID control, while it is around 0.25 degrees in the LQR control. Furthermore, the proposed SMC controller is almost not affected by the disturbance input.

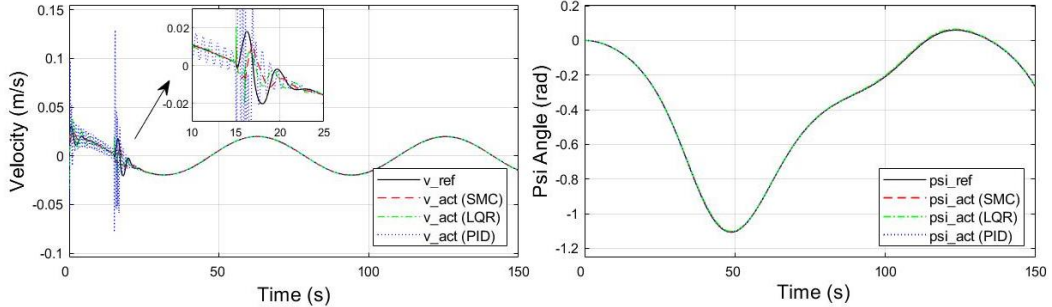


Figure 12. Velocity and movement angle ( $\varphi$ ) of the robot (Case 2)

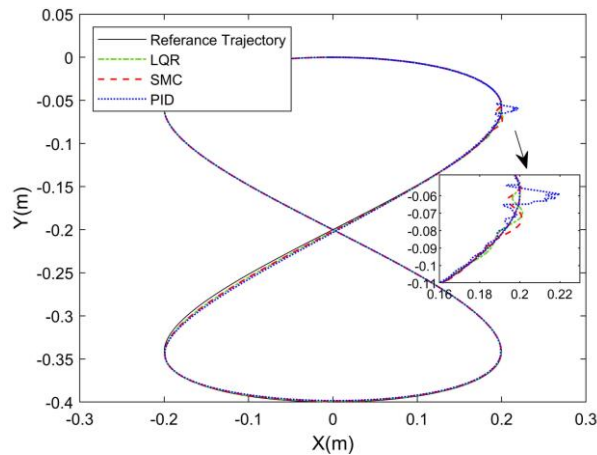


Figure 13. Trajectory Tracking (Case 2)

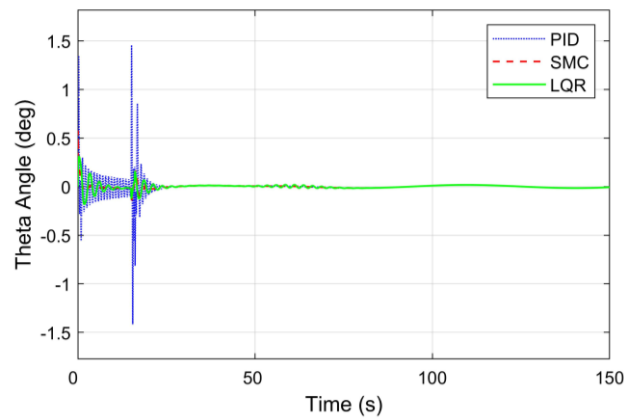


Figure 14. Body ( $\theta$ ) Angle (Case 2)

As seen in Figure 15, although the SMC controller applies much higher torques at the beginning of the movement, it applies much less torque than the PID and LQR controllers against the disturbance input.

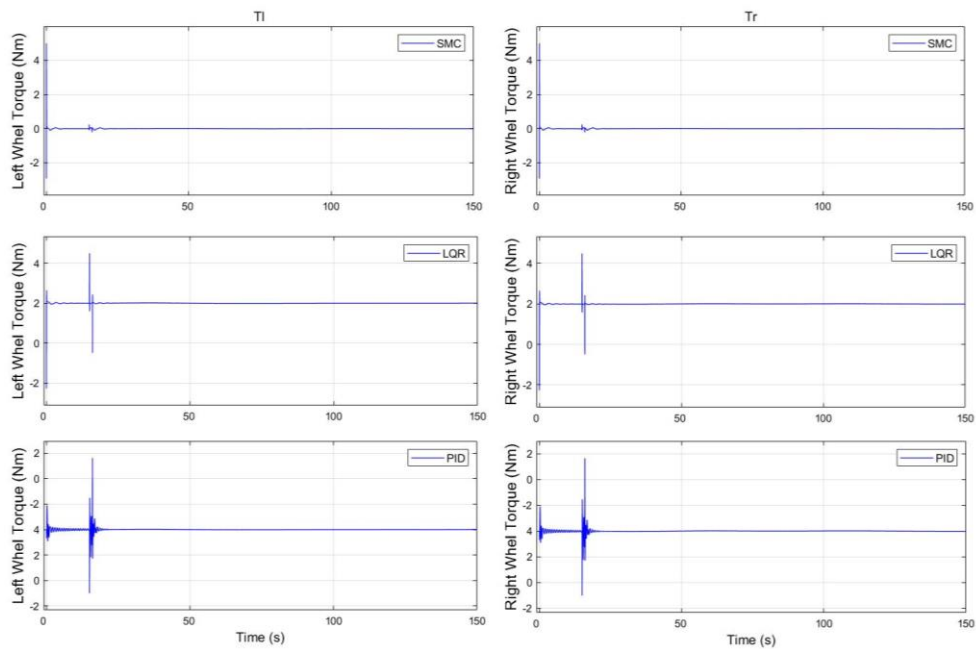


Figure 15. Wheel torques (Case 2)

Parameter uncertainty is a factor affecting the stability of many controllers. In order to test the robustness of the controllers against to parameter uncertainties, simulations were performed by changing the body mass  $M_p$  in three different ways, 6 kg, 10 kg, 50 kg respectively.

**Case 3:** In this case, the body weight  $M_p$  was increased from 3 kg to 6 kg. The PID controller is negatively affected by parameter changes, and it almost lost its stability. Large oscillations in speed, trajectory, and body angle for PID control can be seen in Figure 16- Figure 18.

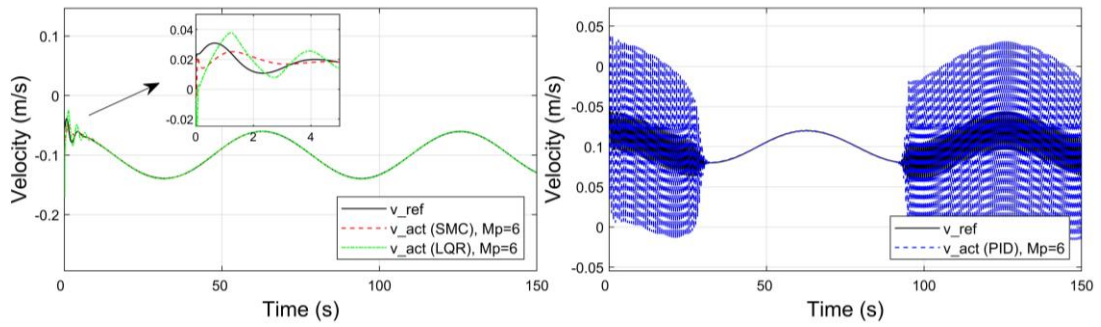


Figure 16. Velocity of the robot (Case 3)

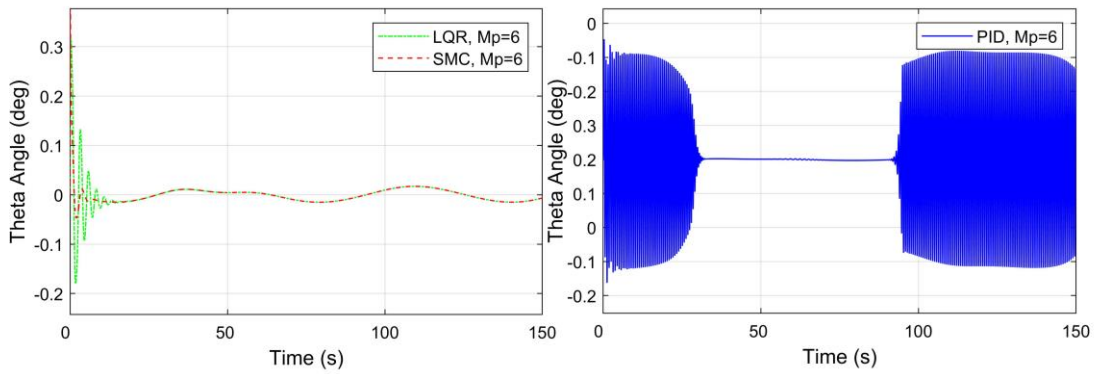


Figure 17. Body ( $\theta$ ) Angle (Case 3)

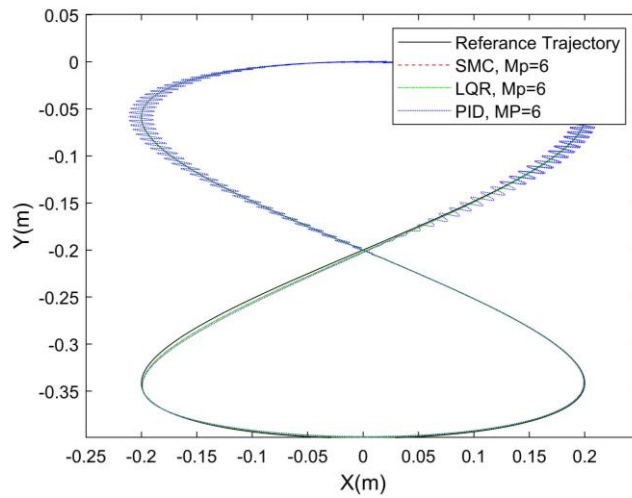


Figure 18. Trajectory Tracking (Case 3)

**Case 4:** Body weight  $M_p$  increased to 10 kg. In this case the PID control response became completely unstable and was therefore not shown in the graphs. On the other hand, it can be seen in Figure 19-Figure 21 that SMC and LQR controllers continue to maintain their stability and offer successful trajectory tracking performance. However, SMC control offers a much more successful performance than LQR in balancing the body angle as seen in Figure 21.

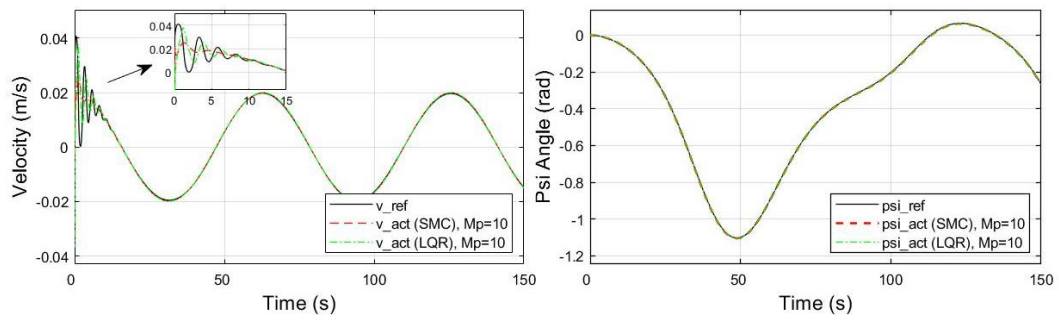


Figure 19. Velocity and movement angle ( $\varphi$ ) of the robot (Case 4)

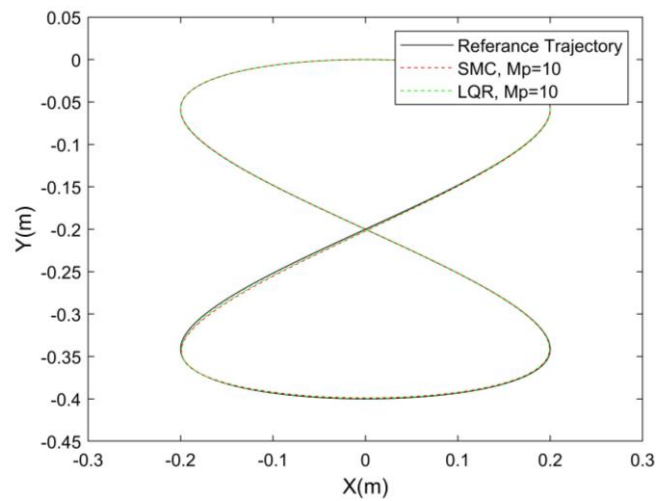


Figure 20. Trajectory Tracking (Case 4)

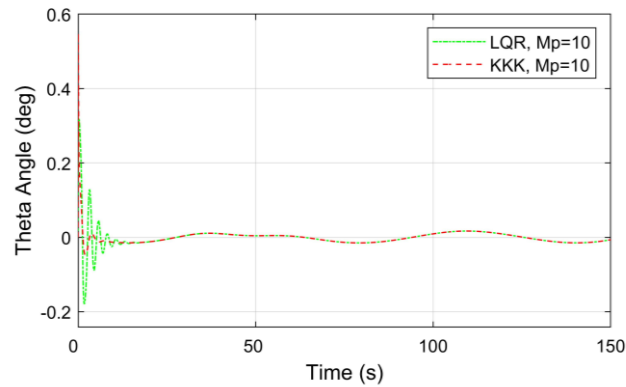


Figure 21. Body ( $\theta$ ) Angle (Case 4)

**Case 5:** In this case the robustness of the proposed controller against to parameter variations was tested under an extreme condition by increasing the body weight  $M_p$  from 3 kg to 50 kg. Under these conditions, it is seen in Figure 22 – Figure 25 that the LQR controller begins to become unstable and excessive oscillations occur in trajectory tracking and body angle. On the other hand, it is seen that the proposed SMC controller maintains its stability even in this extreme case and provides a very successful response in trajectory tracking and balancing the body angle.



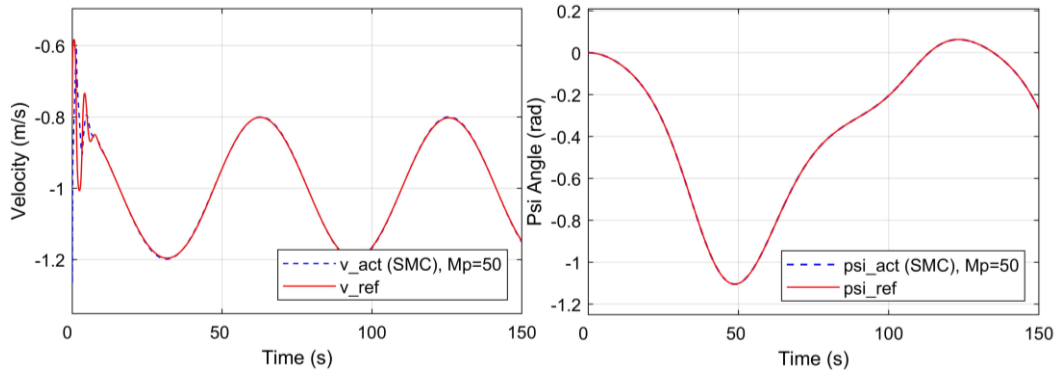


Figure 22. Velocity and movement angle ( $\varphi$ ) of the robot for SMC (Case 5)

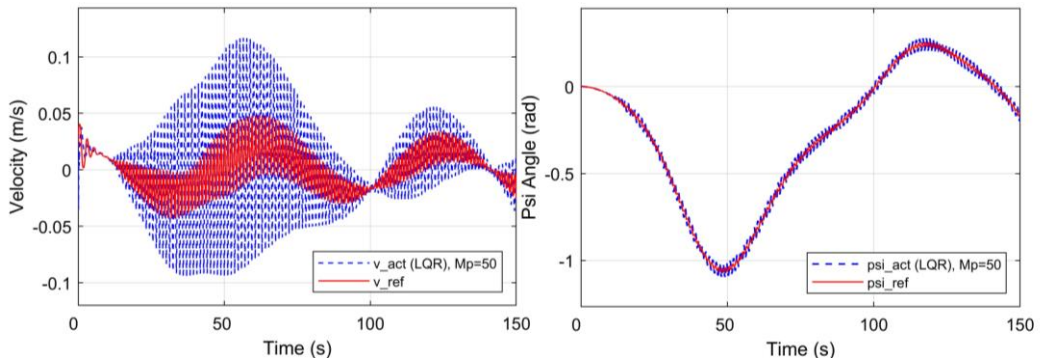


Figure 23. Velocity and movement angle ( $\varphi$ ) of the robot for LQR (Case 5)

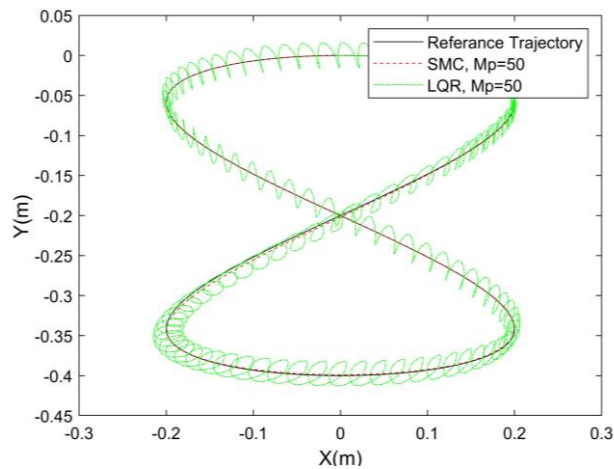


Figure 24. Trajectory Tracking (Case 5)

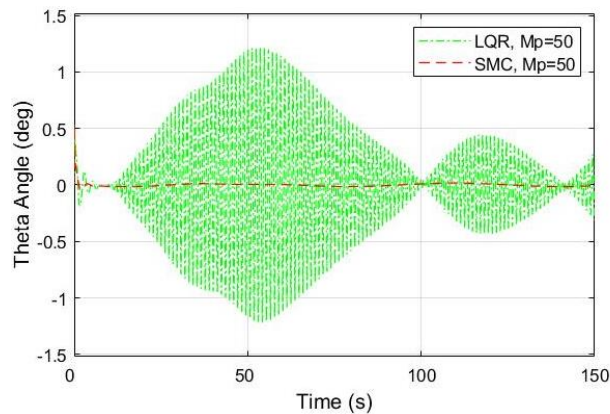


Figure 25. Body ( $\theta$ ) Angle (Case 5)

#### 4. CONCLUSIONS

Parameter uncertainties and external disturbances negatively affect the stability of controllers. In this study, a robust SMC method against to uncertainties and disturbances for trajectory tracking of a two-wheeled self-balancing robot is investigated. In the proposed method, the chattering problem is eliminated by using a tangent hyperbolic switching function. The performance of the proposed method is tested for five different scenarios having different disturbance inputs and parameter changes and compared with LQR and PID controllers. The results showed that the PID control is extremely sensitive to disturbance inputs and parameter changes, and the LQR controller provides a much better performance than the PID control in terms of response speed and robustness. The results also showed that the proposed SMC controller not only offer as good performance as the LQR controller in terms of response speed, but it is extremely robust and almost insensitive to disturbance inputs and excessive parameter changes.

#### Declaration of Ethical Standards

The authors of this article declare that the materials and methods used in this study do not require ethical committee permission and/or legal-special permission.

#### Credit Authorship Contribution Statement

M. DOĞAN: Methodology, Conceptualization, Resources, Investigation, Writing.

U. ÖNEN: Methodology, Conceptualization, Resources, Investigation, Writing -review & editing, Supervision.

#### Declaration of Competing Interest

The authors declare that they have no known competing financial interests or personal relationships that could have appeared to influence the work reported in this paper.

#### Funding / Acknowledgements

The author(s) received no financial support for the research.

#### Data Availability

Data available on request from the author.

#### 5. REFERENCES

- [1] D. Nemeč, D. Adamković, M. Hrubos, R. Pirnik, ve M. Mihalik, "Fast Two-Wheeled Balancing Robot", ss. 1-9, Haz. 2021, doi: 10.1109/ICCC51557.2021.9454659.
- [2] G. C. M. Santo ve C. Garcia, "Construction, Control Design and Bluetooth Trajectory Control of a Self-Balancing Robot", içinde *SBAI 2019*, 2019. doi: 10.17648/sbai-2019-111151.
- [3] K. Prakash ve K. Thomas, "Study of controllers for a two wheeled self-balancing robot", *2016 International Conference on Next Generation Intelligent Systems, ICNGIS 2016*, Şub. 2017, doi: 10.1109/ICNGIS.2016.7854009.
- [4] F. Grasser, A. D'Arrigo, S. Colombi, ve A. C. Rufer, "JOE: A mobile, inverted pendulum", *IEEE Transactions on Industrial Electronics*, c. 49, sy 1, ss. 107-114, Şub. 2002, doi: 10.1109/41.982254.
- [5] M. Velazquez, D. Cruz, S. Garcia, ve M. Bandala, "Velocity and Motion Control of a Self-Balancing Vehicle Based on a Cascade Control Strategy", *Int J Adv Robot Syst*, c. 13, sy 3, Haz. 2016, doi: 10.5772/63933.

- [6] J. X. Xu, Z. Q. Guo, ve T. H. Lee, "Design and implementation of a takagi-sugeno-type fuzzy logic controller on a two-wheeled mobile robot", *IEEE Transactions on Industrial Electronics*, c. 60, sy 12, ss. 5717-5728, 2012, doi: 10.1109/TIE.2012.2230600.
- [7] M. El-Bardini ve A. M. El-Nagar, "Interval type-2 fuzzy PID controller for uncertain nonlinear inverted pendulum system", *ISA Trans*, c. 53, sy 3, ss. 732-743, 2014, doi: 10.1016/J.ISATRA.2014.02.007.
- [8] O. Begovich, E. N. Sanchez, ve M. Maldonado, "Takagi-Sugeno fuzzy scheme for real-time trajectory tracking of an underactuated robot", *IEEE Transactions on Control Systems Technology*, c. 10, sy 1, ss. 14-20, Oca. 2002, doi: 10.1109/87.974334.
- [9] L. Guo, S. A. A. Rizvi, ve Z. Lin, "Optimal control of a two-wheeled self-balancing robot by reinforcement learning", *International Journal of Robust and Nonlinear Control*, c. 31, sy 6, ss. 1885-1904, Nis. 2021, doi: 10.1002/RNC.5058.
- [10] A. Unluturk ve O. Aydogdu, "Machine Learning Based Self-Balancing and Motion Control of the Underactuated Mobile Inverted Pendulum with Variable Load", *IEEE Access*, c. 10, ss. 104706-104718, 2022, doi: 10.1109/ACCESS.2022.3210540.
- [11] H. M. Omar, A. M. Elalawy, ve H. H. Ammar, "Two-wheeled Self balancing robot Modeling and Control using Artificial Neural Networks (ANN)", *NILES 2019 - Novel Intelligent and Leading Emerging Sciences Conference*, ss. 196-200, Eki. 2019, doi: 10.1109/NILES.2019.8909311.
- [12] J. Wu ve S. Jia, "T-S adaptive neural network fuzzy control applied in two-wheeled self-balancing robot", *Proceedings of the 6th International Forum on Strategic Technology, IFOST 2011*, c. 2, ss. 1023-1026, 2011, doi: 10.1109/IFOST.2011.6021194.
- [13] M. Önkol ve C. Kasnakoğlu, "Adaptive model predictive control of a two-wheeled robot manipulator with varying mass", *Measurement and Control (United Kingdom)*, c. 51, sy 1-2, ss. 38-56, Mar. 2018, doi: 10.1177/0020294018758527/ASSET/IMAGES/LARGE/10.1177\_0020294018758527-FIG20.JPEG.
- [14] M. S. Mahmoud ve M. T. Nasir, "Robust control design of wheeled inverted pendulum assistant robot", *IEEE/CAA Journal of Automatica Sinica*, c. 4, sy 4, ss. 628-638, Eki. 2017, doi: 10.1109/JAS.2017.7510613.
- [15] G. V. Raffo, V. Madero, ve M. G. Ortega, "An application of the underactuated nonlinear  $\mathcal{H}_\infty$  controller to two-wheeled self-balanced vehicles", *Proceedings of the 15th IEEE International Conference on Emerging Technologies and Factory Automation, ETFA 2010*, 2010, doi: 10.1109/ETFA.2010.5641024.
- [16] N. Uddin, "Lyapunov-based control system design of two-wheeled robot", *Proceedings - 2017 International Conference on Computer, Control, Informatics and its Applications: Emerging Trends In Computational Science and Engineering, IC3INA 2017*, c. 2018-January, ss. 121-125, Tem. 2017, doi: 10.1109/IC3INA.2017.8251752.
- [17] S. Cheng, H. Liu, ve M. Yao, "An Adaptive Backstepping-Based Controller for Trajectory Tracking of Wheeled Robots", *2021 4th IEEE International Conference on Industrial Cyber-Physical Systems (ICPS)*, ss. 539-544, May. 2021, doi: 10.1109/ICPS49255.2021.9468124.
- [18] L. Jiang, H. Qiu, Z. Wu, ve J. He, "Active disturbance rejection control based on adaptive differential evolution for two-wheeled self-balancing robot", *Proceedings of the 28th Chinese Control and Decision Conference, CCDC 2016*, ss. 6761-6766, Ağu. 2016, doi: 10.1109/CCDC.2016.7532214.
- [19] U. Onen, "Model-Free Controller Design for Nonlinear Underactuated Systems with Uncertainties and Disturbances by Using Extended State Observer Based Chattering-Free Sliding Mode Control", *IEEE Access*, c. 11, ss. 2875-2885, 2023, doi: 10.1109/ACCESS.2023.3234864.
- [20] V. T. Nguyen, C. Y. Lin, S. F. Su, ve Q. V. Tran, "Adaptive Chattering Free Neural Network Based Sliding Mode Control for Trajectory Tracking of Redundant Parallel Manipulators", *Asian J Control*, c. 21, sy 3, ss. 1-16, Mar. 2019, doi: 10.1002/ASJC.1789.

- [21] W. Junfeng ve Z. Wanying, "Research on control method of two-wheeled self-balancing robot", *Proceedings - 4th International Conference on Intelligent Computation Technology and Automation, ICICTA 2011*, c. 1, ss. 476-479, 2011, doi: 10.1109/ICICTA.2011.132.
- [22] F. N. Martins, M. Sarcinelli-Filho, ve R. Carelli, "A Velocity-Based Dynamic Model and Its Properties for Differential Drive Mobile Robots", *Journal of Intelligent and Robotic Systems: Theory and Applications*, c. 85, sy 2, ss. 277-292, Şub. 2017, doi: 10.1007/S10846-016-0381-9/METRICS.
- [23] D. Qian ve J. Yi, *Hierarchical Sliding Mode Control for Under-actuated Cranes*. Springer Berlin Heidelberg, 2015. doi: 10.1007/978-3-662-48417-3.
- [24] M. Tinkir, U. Onen, M. Kalyoncu, ve F. M. Botsali, "Pid and interval type-2 fuzzy logic control of double inverted pendulum system", *2010 The 2nd International Conference on Computer and Automation Engineering, ICCAE 2010*, c. 1, ss. 117-121, 2010, doi: 10.1109/ICCAE.2010.5451988.
- [25] O. Çakır, ve S. Tekin, "Oransal İntegral Türevsel Denetleyici Parametrelerinin Sezgisel Optimizasyon Yöntemleri ile Ayarlanması", *Avrupa Bilim ve Teknoloji Dergisi*, sy 23, ss. 9-21, Nis. 2021, doi: 10.31590/EJOSAT.830467.
- [26] Ü. Önen, A. Çakan, ve İ. İlhan, "Particle Swarm Optimization Based LQR Control of an Inverted Pendulum", *ETJ Engineering and Technology Journal*, c. 2, ss. 2456-3358, 2017, doi: 10.18535/etj/v2i5.01.